The Sixteenth International Symposium on Artificial Life and Robotics 2011 (AROB 16th '11),
B-Con Plaza, Beppu,Oita, Japan, January 27-29, 2011

Subsurface imaging for anti-personal mine detection by Bayesian super-resolution with Smooth-gap prior

Satoshi Kozawa, Takashi Takenouchi and Kazushi Ikeda

Nara Institute of Science and Technology
8916-5 Takayama, Ikoma, Nara, Japan
Phone: +81-0743-72-5986, E-mail: {satoshi-ko,ttakashi,kazushi}@is.naist.jp

Abstract: Ground penetrating radars (GPRs) have been studied to reconstruct a subsurface image. Signal observed by the GPRs typically includes very strong noise and reconstruction of the image is a difficult task. We propose a new subsurface imaging method based on the framework of the Bayesian super-resolution. In the framework, we can incorporate additional information into the reconstructed image by considering a smooth-gap prior, which can represent smoothness of the subsurface image and gaps between materials, and improves the quality of the reconstructed image. We investigated performance of the proposed method with a synthetic GPR dataset, and confirmed the validity of the proposed method.

Keywords: Subsurface Imaging, Inverse problems, Smooth-gap prior

1. Introduction

In the past, anti-personnel mines were mainly made from metals and hence metal detectors were typical tools for detecting buried anti-personnel mines. However, recent plastic mines are difficult to detect because they include few metal parts. Highly sensitive metal detectors may enable us to find plastic mines, but they also induce high false detection error caused by small metallic pieces such as nails or cans. To overcome this difficulty, ground penetrating radars (GPRs) have been studied. A GPR transmits electromagnetic waves into a ground surface, observes the reflected waves, and reconstructs an image that represents the condition of the ground subsurface. An observed signal includes very strong noise that degrades the quality of the reconstructed image and the performance of detection. To improve the image quality, some methods for subsurface imaging with GPRs have been proposed.

Feng and Sato [1] tried to reconstruct the subsurface image by applying the pre-stack migration (which is a subsurface imaging method) for synthetic aperture radars (SARs). A SAR has two or more antennas that transmit or receive electromagnetic waves. The method improves the image quality and shows clear shapes of objects, however, still has noise in the reconstructed image, and the resultant image causes high false positive error for mine detection. Gurbuz *et al*. [2] formulated the imaging problem as an inverse problem based on the model used in [1], and applied the Dantzig selector, which assumes sparseness with respect to the existing probability of buried objects. The assumption of the sparseness is a kind of regularization for the inverse problem, and the method for reconstructing images is more informative for specification of the location of subsurface objects. However, the reconstructed images lose information on the shapes of objects, which makes it difficult to distinguish mines from other objects.

We propose a new subsurface imaging method based on the Bayesian inference. In the Bayesian framework, we can incorporate additional information into the reconstructed image by considering a smooth-gap prior. The prior can describe smoothness of the subsurface image as well as gaps between materials, by introducing binary latent variables representing whether there is a gap or not between two points. However calculation of the posterior distribution using the prior is not computationally feasible because marginalization of latent variables for all pair of points requires exponential computation time. To overcome the difficulty, we employ the Variational-Bayes (VB) method, in which the posterior is assumed to be written in a factorized form. We investigated performance of the proposed method with a synthetic GPRs datasets, and confirmed the validity of the proposed method.

2. Bayesian Framework

The GPRs use electromagnetic waves to explore the subsurface of the target. In this paper, we consider a bistatic GPR, which has two antennas, one of which transmits electromagnetic waves and the other receives the reflected waves. For subsurface imaging, the GPRs observe the reflected signals $\mathbf{y}_k \in \mathrm{R}^{N_t}$ at k-th scan points and are moved to the next scan point; and as a whole, a dataset $\{\mathbf{y}_k\}_{k=1}^{K}$

is observed. We assume that the transmitted waves are reflected at only the boundary of two materials with different dielectric constants and then the received signals include information on the boundary in the subsurface. Additionally, we assume that the observed signals at the scan point are represented as a linear superposition of reflected signals from points over the boundary at a scan point. In a practical sense, there are interactions among the reflected signals from points in the subsurface and then the assumption of linear superposition cannot be appropriate; however, we use the model for simplicity.

Let us consider a physical model that represents a relationship between the received signal reflected from a point p and the transmitted signal $s(t)$ as

$$\zeta_{k,p}(t) = \frac{\sigma_p s(t-\tau_k(p))}{A_{k,p}} \tag{1}$$

where $\zeta_{k,p}(t)$ is the received signal reflected from the point p in the subsurface at the k-th scan point, $\tau_k(p)$ is the total round-trip delay between the antennas and the target point p at the k-th scan point, σ_p is the reflection coefficient of the target point and $A_{k,p}$ is a scaling factor accounting for loss of the signal. Note that the reflection coefficient is positive when the target point p is on the boundary of two materials with different dielectric constants, and otherwise is zero. A whole model of the observed signal $d_k(t)$ at k-th scan point is the superposition of reflected signals and then is written as

$$d_k(t) = \iiint_\Omega \zeta_k(x,y,z,t)dxdydz \tag{2}$$

where Ω is a target region of interest. This is called the point-target model [1][2].

To calculate the right hand side of (2), we discretize the integration in (2) as follows:

$$d_k(t_i) = \sum_{j=1}^{N} s(t_i-\tau_k(j))\frac{\sigma(j)}{A(k,j)} \tag{3}$$

where j is an index of a discretized point in the target region Ω, $t_i = t_0 + i/Fs$, t_0 is an initial time of measurement and Fs is a sampling frequency. We observe that a vector $\mathbf{d}_k = (d_k(t_0), \ldots, d_k(t_{N_t-1}))^t$ of $d_k(t)$ is written as

$$\mathbf{d}_k = \mathbf{W}_k\mathbf{x} \tag{4}$$

where $\mathbf{x}$ is an N-dimensional vector whose n-th element is $\sigma(n)/A(k,n)$ and $\mathbf{W}_k$ is a matrix whose (i,j) component is

$$\mathbf{W}_k(i,j) = s(t_i - \tau_k(j)) \tag{5}$$

Here we assume that the GPRs measurement data at k-th scan point is represented as

$$\mathbf{y}_k = \mathbf{W}_k\mathbf{x} + \boldsymbol{\epsilon} \tag{6}$$

where $\boldsymbol{\epsilon}$ is measurement noise. Note that the n-th element of $\mathbf{x}$ represents a reflectivity profile corresponding to the n-th point in the target subsurface space. In other words, $\mathbf{x}$ corresponds to the subsurface image itself of the target space and then our goal is to estimate $\mathbf{x}$ using the observed dataset $\{\mathbf{y}_k\}_{k=1}^K$.

2.1. Probabilistic formulation

We assume that a probability distribution of the measurement noise $\boldsymbol{\epsilon}$ is given by an isotropic Gaussian with a mean vector $\mathbf{0}$. Then a conditional distribution of $\mathbf{y}_k$ given $\mathbf{x}$ is written as

$$\begin{aligned} p(\mathbf{y}_k|\mathbf{x}) &= \mathcal{N}(\mathbf{y}_k|\mathbf{W}_k\mathbf{x}, \beta^{-1}\mathbf{I}), \quad (7)\\ &= \frac{1}{Z}\exp\left(-\frac{\beta}{2}||\mathbf{y}_k - \mathbf{W}_k\mathbf{x}||^2\right) \quad (8)\end{aligned}$$

where β is a prediction parameter and Z is a normalization constant. As a prior distribution of $\mathbf{x}$, we employ the following smooth-gap prior distribution [3]

$$p(\mathbf{x}) = \sum_{\boldsymbol{\eta}} p(\mathbf{x},\boldsymbol{\eta}), \tag{9}$$

$$p(\mathbf{x},\boldsymbol{\eta}) = \frac{1}{Z}\exp\left(-\frac{\rho}{2}E(\mathbf{x},\boldsymbol{\eta})\right) \tag{10}$$

where $\boldsymbol{\eta}$ is a vector of binary latent variables, each of which represents the gap between two materials, ρ is a hyper parameter that controls the strengh of the effect of the prior distribution, and E is an energy function defined as follows:

$$E(\mathbf{x},\boldsymbol{\eta}) = \sum_{i\sim j}\left(\eta_{ij}(x_i-x_j)^2 + (1-\eta_{ij})\lambda\right). \tag{11}$$

The summation $\sum_{i\sim j}$ is taken over all pairs of neighboring pixels. The latent variable η_{ij} represents the local characteristics of the prior and indicates whether a pair of pixels take similar values or not. When $\eta_{ij} = 1$, the pixels i and j are smoothed due to the quadratic penalty, and there is no effect for the smoothing when $\eta_{ij} = 0$. Thus, this prior controls
whether there is a gap or not between two materials by the latent variable $\boldsymbol{\eta}$.

We can rewrite the joint distribution (10) as

$$p(\mathbf{x},\boldsymbol{\eta}) = p(\mathbf{x}|\boldsymbol{\eta})p(\boldsymbol{\eta}) \tag{12}$$

where,

$$p(\boldsymbol{\eta}) = \mathrm{Ber}(\boldsymbol{\eta}|\nu), \tag{13}$$

$$p(\mathbf{x}|\boldsymbol{\eta}) = \mathcal{N}(\mathbf{x}|\mathbf{0}, \rho^{-1}A_{\boldsymbol{\eta}}^{-1}). \tag{14}$$

Here, $\nu = 1/(1+\exp(-\lambda\rho/2))$ is a parameter for the Bernoulli distribution $\mathrm{Ber}(\boldsymbol{\eta}|\nu) = \prod_{i\sim j} \nu^{\eta_{ij}}(1-\nu)^{1-\eta_{ij}}$, and (i,j) component of a matrix $A_{\boldsymbol{\eta}}$ is defined by

$$[A_{\boldsymbol{\eta}}]_{ij} = \begin{cases} \sum_{k\in N(i)} \eta_{ik}, & i=j, \\ -\eta_{ij}, & i\sim j, \\ 0, & \text{otherwise}, \end{cases} \quad (15)$$

where $N(i)$ is the set of neighboring pixels of the pixel i. Then the posterior can be strictly calculated as follows:

$$\begin{aligned} p(\mathbf{x}|\{\mathbf{y}_k\}_{k=1}^K) &= \frac{p(\mathbf{x})\prod_{k=1}^K p(\mathbf{y}_k|\mathbf{x})}{p(\{\mathbf{y}_k\})} & (16) \\ &= \sum_{\boldsymbol{\eta}} p(\boldsymbol{\eta}|\{\mathbf{y}_k\})\mathcal{N}(\boldsymbol{\mu}_{\boldsymbol{\eta}}, \boldsymbol{\Sigma}_{\boldsymbol{\eta}}), & (17) \end{aligned}$$

where

$$\begin{aligned} \boldsymbol{\Sigma}_{\boldsymbol{\eta}} &= \left[\rho A_{\boldsymbol{\eta}} + \beta\left(\sum_{k=1}^K \mathbf{W}_k^t \mathbf{W}_k\right)\right]^{-1}, & (18) \\ \boldsymbol{\mu}_{\boldsymbol{\eta}} &= \beta\boldsymbol{\Sigma}_{\boldsymbol{\eta}}\left(\sum_{k=1}^K \mathbf{W}_k^t \mathbf{y}_k\right). & (19) \end{aligned}$$

We employ the maximum *a posteriori* (MAP) estimate $\sum_{\boldsymbol{\eta}} p(\boldsymbol{\eta}|\{\mathbf{y}_k\})\boldsymbol{\mu}_{\boldsymbol{\eta}}$ of (16) for the estimated of subsurface image $\hat{\mathbf{x}}$. However, since this estimate has the summation over all pairs of neighboring pixels, it requires exponential order of computational complexity and hence it is impossible to explicitely compute the estimate. To cope with this problem, we employ Variational-Bayes (VB) method to approximate the posterior in this study.

2.2. Variational-Bayes method

For the VB approximation, we introduce a trial distribution $q(\mathbf{x},\boldsymbol{\eta})$ which maximizes the variational-energy function

$$F(q) = \sum_{\boldsymbol{\eta}} \int q(\mathbf{x},\boldsymbol{\eta}) \ln \frac{p(\mathbf{x},\boldsymbol{\eta},\{\mathbf{y}_k\})}{q(\mathbf{x},\boldsymbol{\eta})} \mathrm{d}\mathbf{x}. \quad (20)$$

The trial distribution can approximate $p(\mathbf{x},\boldsymbol{\eta}|\{\mathbf{y}_k\})$ since maximization of the variational-energy function with respect to q is equivalent to minimization of Kullback-Leibler divergence between $p(\mathbf{x},\boldsymbol{\eta}|\{\mathbf{y}_k\})$ and $q(\mathbf{x},\boldsymbol{\eta})$. Although the trial distribution can be an arbitrary probability distribution for the unknown variables $\mathbf{x}$ and $\boldsymbol{\eta}$ in principle, for the sake of tractability, we assume that it can be factorized as:

$$q(\mathbf{x},\boldsymbol{\eta}) = q_{\mathbf{x}}(\mathbf{x}) \prod_{i\sim j} q_{\eta_{ij}}(\eta_{ij}). \quad (21)$$

Under the assumption, the optimal trial distribution maximizing (20) is analytically given as

$$q_{\mathbf{x}}^*(\mathbf{x}) = \mathcal{N}(\mathbf{x}|\boldsymbol{\mu},\Sigma) \quad (22)$$

where

$$\begin{aligned} \Sigma &= \left(\rho\mathbb{E}_{\boldsymbol{\eta}}[A_{\boldsymbol{\eta}}] + \beta\sum_{k=1}^K W_k^t W_k\right)^{-1}, & (23) \\ \boldsymbol{\mu} &= \Sigma\left(\beta\sum_{k=1}^K W_k^t y_k\right), & (24) \end{aligned}$$

and,

$$q_{\eta_{ij}}^*(\eta_{ij}) = \mathrm{Ber}(\eta_{ij}|\nu_{ij}) \quad (25)$$

where

$$\nu_{ij} = \frac{1}{1+\exp(-\frac{\rho}{2}(\lambda - \mathbb{E}_{\mathbf{x}}[(x_i-x_j)^2]))}. \quad (26)$$

We employ μ in (22) as the approximated variable of the estimated subsurface image $\mathbf{x}$.

3. Experiments

In this section, we examined performance of the proposed methods by comparing with the existing methods (Feng and Sato [1] and Gurbuz [2]) using a synthetic GPR dataset. We created a target space as shown in Fig. 1(a): three objects (rectangle, diamond shape, "O") are buried in the target space. The GPR space-time observation $\{\mathbf{y}_k\}_{k=1}^K$ is generated by (6), in which the SNR is 15 dB. In this experiment, the transmitter-receiver distance is 10 cm and both antennae are a height of 10 cm. The number K of GPR scan points is 400 and an interval of each scan point is uniform.

Results by the Feng and Sato method, and the Gurbuz method are shown in Fig. 1(b) and (c), respectively. In our Bayesian approach, we applied three kinds of prior distributions, the non-informative prior, the smooth prior [4] and the smooth-gap prior defined by (9). The non-informative prior is given by $p(\mathbf{x}) = \mathcal{N}(\mathbf{x}|\mathbf{0}, Z^{-1})$ with a precision matrix $Z^{-1} = \mathbf{0}$, whose posterior mean is written as $\hat{\mathbf{x}} = (\sum_{k=1}^K \mathbf{W}_k^t\mathbf{W}_k)^{-1}\sum_{k=1}^K \mathbf{W}_k^t\mathbf{y}_k$. The smooth prior is a special case of (9) and is given by setting $\eta_{ij} = 1(\forall i,j)$, which results in $\hat{\mathbf{x}} = (\rho A_{\boldsymbol{\eta}}|_{\boldsymbol{\eta}=\mathbf{1}} + \beta\sum_{k=1}^K \mathbf{W}_k^t\mathbf{W}_k)^{-1}\beta\sum_{k=1}^K \mathbf{W}_k^t\mathbf{y}_k$. Figure 1(d), (e) and (f) respectively show the reconstructed subsurface images with the non-informative prior, the smooth prior ($\beta = 0.1$, $\rho = 1.0$) and the smooth-gap prior ($\lambda = 0.04$, $\beta = 0.1$, $\rho = 1$). While the proposed method with the non-informative prior (Fig. 1(d)) failed to reconstruct the subsurface image,the proposed method with the smooth prior (Fig. 1(e)) and the smooth-gap prior (Fig. 1(f)) could reconstruct the subsurface image by which we can recognize shapes of three buried objects. Also, Fengs method (Fig. 1(b)) could reconstruct the image; however, boundaries of target objects

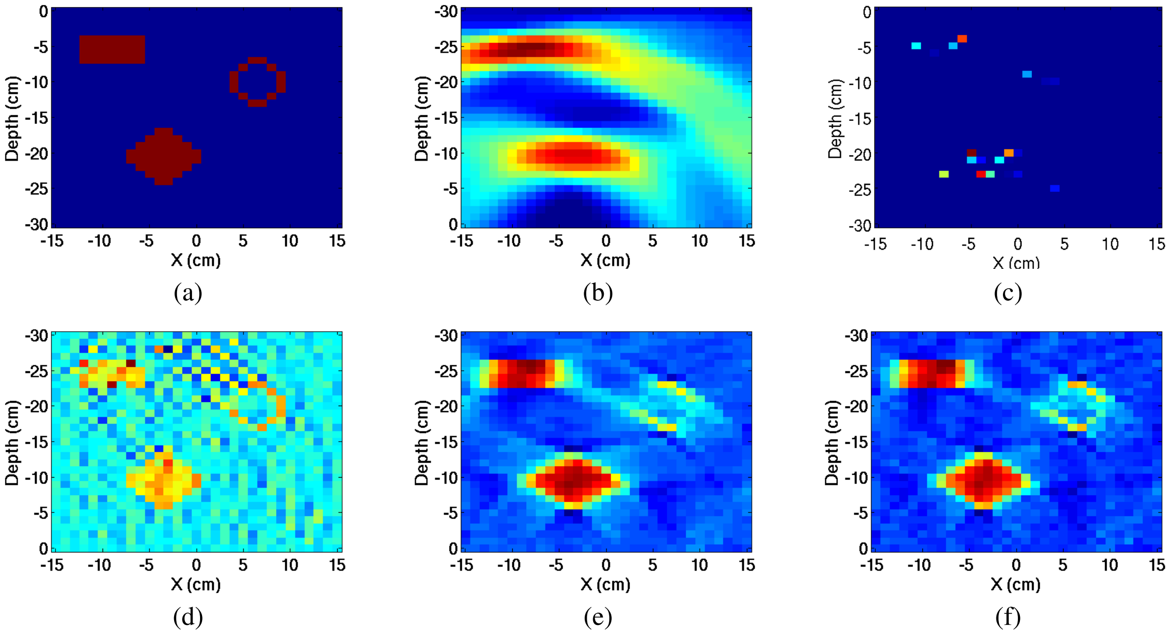

Figure 1: (a) Target space in which three objects are buried: Horizontal axis represents a spatial position in a lateral direction and vertical axis represents the depth. (b) Feng and Sato method, (c) Gurbuz method, (d) Proposed method with the non-informative prior, (e) Proposed method with the smooth prior, (f) Proposed method with the smooth-gap prior

were obscure compared with Fig. 1(e), (f), and we cannot find the object shaped like a "O". The resultant image by the Gurbuz method in Fig. 1(c) distinctly indicated points of existing objects because of the assumption of the sparseness with respect to the existing probability of buried objects. However, information on shapes of buried objects was lost and it is difficult to determine whether the detected object is a landmine or not.

To investigate the quality of the reconstructed subsurface image, we calculate a normalized SNR of the image reconstructed by the proposed method, with the smooth prior and the smooth-gap prior, and the method of Feng and Sato, respectively. We define a normalized SNR between the true subsurface image and the reconstructed image as

$$10 \log_{10} \frac{||\mathbf{x}_{true}/ \max \mathbf{x}_{true}||^2}{||\hat{\mathbf{x}}/ \max \hat{\mathbf{x}} - \mathbf{x}_{true}/ \max \mathbf{x}_{true}||^2} \text{ [dB]} \quad (27)$$

where $\mathbf{x}_{true}$ is a vector associated with Fig. 1(a) and $\hat{\mathbf{x}}$ is an estimated vector. The result of Feng and Sato method is -1.96 dB, Gurbuz method -0.119 dB, and the results of the proposed method with the smooth prior and the smooth-gap prior are 5.96 dB and 6.176 dB, respectively. Then we observe that the proposed method significantly outperformed the method of Feng and Sato, and also, the smooth-gap prior which can represent gap information, improved performance compared to the smooth prior.

4. Conclusion

In this paper, we proposed a new subsurface imaging method based on Bayesian framework which enables us to use prior knowledge such that represents the smoothness of the subsurface and the gap between two materials. We observed that the proposed method attained better performance compared with conventional methods for the synthetic dataset. Application of the proposed method for real datasets will be a future work.

References

[1] X. Feng and M. Sato: Pre-stack migration applied to GPR for landmine detection, Inverse Problems, Vol. 20, pp. 99-115, 2004.

[2] A.C. Gurbuz, J.H. McClellan and W.R. Scott Jr: Compressive sensing for subsurface imaging using ground penetrating radar, Signal Processing, Vol. 89, pp. 1959-1972, 2009.

[3] A. Kanemura, S. Maeda and S. Ishii: Super-resolution with smooth-gap prior, IEICE Technical Report. (NC), Vol. 105, No. 130, pp. 31-36, 2005.

[4] S. Kozawa, T. Takenouchi, I. Kazushi: Subsurface imaging by Bayesian super-resolution for anti-personal mine detection using ground penetrating radar, Journal of Signal Processing, Vol. 14, No. 4, 2010.